Multi-objective optimization of the engine performance and emissions for a hydrogen/gasoline dual-fuel engine equipped with the port water injection system

Farhad Salek[1], Meisam Babaie *[2], Seyed Vahid Hosseini[1], O. Anwar Bég[2]

[1]Faculty of Mechanical and Mechatronic Engineering, Shahrood University of Technology, Shahrood, Iran

[2]School of Science, Engineering and Environment, University of Salford, Manchester, UK

Abstract

Hydrogen is one of the most promising options being considered as the fuel of future. However, injection of hydrogen into modern gasoline fueled engines can cause some issues such as power loss. This study, therefore, aims to address this challenge in a simulated hydrogen/gasoline dual-fueled engine by developing a novel and innovative approach without possible side effects such as NOx increment. To achieve this goal, the impacts of water injection and the start of the combustion (SOC) modification in a gasoline/hydrogen duel fueled engine have been rigorously investigated. In current methodology, an engine is simulated using AVL software and the model is validated against the experimental data. The Latin Hypercube design experiment method was employed to determine the design points in 3-dimensional space. Due to the existing trade-off between NOx and BMEP, multi-objective optimization using genetic algorithm (GA) was implemented to determine the optimum values of water injection and SOC in various hydrogen energy shares and the effects of optimum design parameters on the main engine performance and emission parameters were investigated. The results showed that the proposed solution could recover the brake mean effective pressure (BMEP) and in some hydrogen energy shares even increase it above the level of single

fueled gasoline engine with the added benefit of there being no increase in NOx compared to the original level. Furthermore, other emissions and engine performance parameters are improved including the engine equivalent Brake specific fuel consumption (BSFC) which was shown to increased up to 4.61%.

Keywords: *Hydrogen/gasoline dual fueled engines; Latin Hypercube design experiment method; Multi-objective optimization; BMEP; BSFC.*

1. Introduction

Emission reduction from internal combustion (IC) engines is a major challenge for the transport sector (1). To overcome this issue, the automotive industry has implemented a variety of different technological solutions for emission reduction and a concerted shift towards electrification of the powertrain system (2). Recently, different types of hybrid and electric vehicles such as Hybrid Electric Vehicles (HEVs), Battery Electric vehicles (BEVs) and Fuel Cell Hybrid Electric Vehicles (FCHEVs) have been introduced with the aim of reducing emissions. However, there are still numerous challenges facing electric vehicles including the low energy density of Lithium-ions, heavy battery weight and high capital cost as well as the limitation of Lithium resources and environmental concerns of mining (3). Furthermore, phasing-out the IC engines could take a decade or so in Europe while it would be slower in developing countries. In light of this, evidently, IC engines have a long life ahead even for road transport. Consequently, electrification cannot be viewed as the *only* solution for resolving the emissions of modern transportation systems. Other options such as dual fuel systems could be considered for conventional IC engines in which the injection of an auxiliary fuel can reduce the fuel consumption and improve the engine performance by emitting less pollutions (4, 5). Recently, hydrogen has been proposed as the green fuel of the future (6, 7). Hydrogen oxidation will not generate any chemical pollutant (8), and is therefore a viable alternative for fossil fuels in vehicles. However, there are some conceptual issues for running IC engines with 100% hydrogen and major modifications are needed in the engine. Instead, for an intermediate solution, hydrogen can be employed as an auxiliary fuel in vehicles with the goal of reduction in fuel consumption and emissions(9, 10). For instance, in a recent study by Zhou et al. (11), it was shown that adding hydrogen to the vehicle fuel can lead to reduction of fuel consumption price and the emission production rate.

As reported by different researchers (12-14, 15 , 16, 17), engine performance is significantly affected by hydrogen injection due to its high flammability and heating value. Geca and Litak (18) measured engine peak pressure fluctuations by injecting hydrogen as the secondary fuel for various energy shares of hydrogen ranging from 5% to 20%. The in-cylinder peak pressure fluctuation affected the dynamical combustion process due to the existence of hydrogen content in the combustion chamber (17). When the air-fuel ratio is fixed, a reduction of engine thermal efficiency, engine power and NOx emission with hydrogen injection were concluded (11, 17). As reported by Magryta (15) and Ji (19), injecting hydrogen by various *energy shares* into the engine results in a decrease in engine thermal efficiency, power output and NOx emissions. The reduction in engine power could be avoided when changing the air to fuel ratio by adding the hydrogen as an extra fuel as reported by Kim et al. (12). According to their experimental results, adding hydrogen can improve the engine thermal efficiency, however, the increase in NOx was also reported by hydrogen injection in this study due to the increase in combustion temperature.

Water injection and ignition timing modification can overcome the challenge of power reduction by hydrogen injection and successfully reduce NOx emission (18, 20-24). Start of combustion (or spark timing) is an important parameter which can affect the performance of the hydrogen-gasoline fueled engines (18 , 21, 25, 26). The engine ignition timing should be modified when hydrogen is to be injected into the engine since it significantly affects the engine emissions and thermal efficiency (27, 28). Water injection is also a solution for NOx reduction as recommended by Chintala *et al.* (29) in a study for simultaneous water and hydrogen injection into the engine. Hydrogen and oxygen mixture were injected into the engine at various volumetric flow rates and water was added into the engine intake manifold with the goal of NOx reduction in this study. Based on their results, it was found that water injection reduced the engine NOx emission by approximately 60%; however, the HC was increased. Another similar study was accomplished by Dhyani et al (28) on controlling the NOx generation rate and backfire in a spark ignition engine. As it is reported by them, injection of water into the engine resulted in significant reduction of engine NOx production rate, and it is recommended an effective way for controlling the backfire during the combustion. The impacts of co-injection of water and hydrogen on performance and emission production of a spark ignition engine fueled by natural gas was studied by Wang et al (22). In this research, the engine was modeled by a 2D engine modelling software. The results showed that injection of water reduce the engine power and NOx emissions. Furthermore, it was also reported that engine HC and CO production rates were increased due to the reduction of the combustion chamber temperature.

Numerical analysis of engine performance is a common practice in modern automotive engineering. For example, a numerical 2-D study was employed by Ji *et al*. (27) and Magryta *et al.* (15) and other researchers (30-33) for simulating hydrogen addition into the engine. It was shown in both studies that the results from numerical simulation in AVL simulation software has a strong agreement with experimental data. Furthermore, the negative impacts of adding hydrogen on engine thermal and volumetric efficiencies were confirmed by Magryta *et al*. (15). Furthermore, in many relevant studies, design of experiment methods such as response surface methodology have been used to investigated the effects of adding different fuels on engine performance and emissions (34-36). Employment of design of experiment methods in experiments and numerical analysis of engines results in figuring out the mathematical relation between design (or functional) parameters and engine various outputs. In addition, the regression analysis can be employed to define an equation for each response in DOE methods which can be used in optimization process (34).

As discussed above, the injection of hydrogen into the engine at *fixed air to fuel ratio* will incur some negative effects on the engine performance such as reduction of thermal efficiency and power (15, 27). Injection of water and modification of the SOC angle are two efficient ways for increasing the power (18, 21, 23, 24, 27, 29, 37), so they can be employed for hydrogen-gasoline fueled engines. However, the potential of water injection and SOC in improving the power loss resulted from hydrogen injection as well as the engine thermal efficiency has not been investigated. In this study, the *novel idea of water injection and tuning the SOC are proposed for a hydrogen-gasoline fueled engine in which the hydrogen is injected with various energy shares*. To overcome the challenge of power loss and realized the environmental benefits of hydrogen injection, the aim is to optimize the engine *BMEP and NOx* based on water injection rate and start of combustion (SOC) at different hydrogen energy shares. To achieve this aim, the engine has been simulated with AVL BOOST software and validated against the experimental data. The Latin Hypercube design of experiment method was employed to determine the design points in 3D space. Three design variables have been considered in this study: *H_2 energy share, water injection ratio (WIR) and start of combustion (SOC)* in the model with two objective functions, i.e. *BMEP and NOx*. A regression analysis has been utilized to provide the equations required in the optimization process for the objective functions. To establish the *optimum values* of water injection and SOC angle for each hydrogen energy share, multi-objective optimization using Genetic algorithm (GA) is deployed. Next, the engine performance is evaluated at the optimum point for the engine rated condition (6000 RPM). To demonstrate the effectiveness of the proposed method, the optimized engine has further been compared with hydrogen-gasoline fueled engine and original single gasoline fueled engine for several engine performance and emission criteria.

2. Methodology

2.1 Experimental set-up

Figure 1 shows the engine test bed and the related eddy current dynamometer. The schematic diagram of engine test bed is also presented in **Figure 2**. The test bed was developed for a KIA Cerato engine which is the case study of this research. The KIA Cerato engine specifications are presented in **Table 1**. Initially, the engine was tested at various operating conditions to collect the experimental data used for validating the model. The engine tests were performed in steady state condition at rated RPM. The main engine functional parameters such as fuel consumption rate (for calculation of BSFC), engine torque and NOx emission were measured and used for validation of the mathematical model in this research.

At engine test room, the Schenck 190 kW dynamometer was employed to run the engine for collecting the data at different RPMs. During the experiments, the engine functional parameters were recorded and used for validation of engine mathematical model which is explained in following sections. The engine test standard code and laboratory testing and calibration standard code are ISO 1585 and ISO 17025, respectively. Moreover, the uncertainty analysis of testing instruments is presented in **Table 2**.

Table.1 Specifications of KIA Cerato engine

Parameter	Unit	Value
Bore	mm	86
Stroke	mm	86
Connecting rod length	mm	143.5
Number of Cylinders		4
Maximum Power	kW	92
Maximum RPM	RPM	7000
Rated RPM	RPM	6000
Compression Ratio		10.5

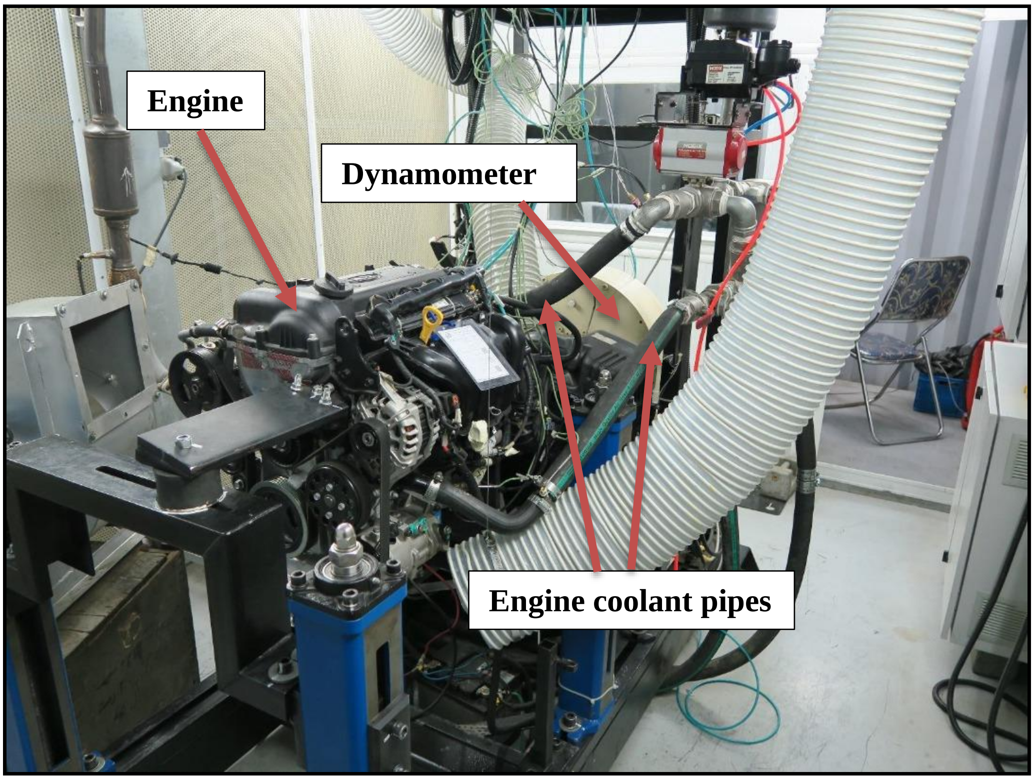

(a)

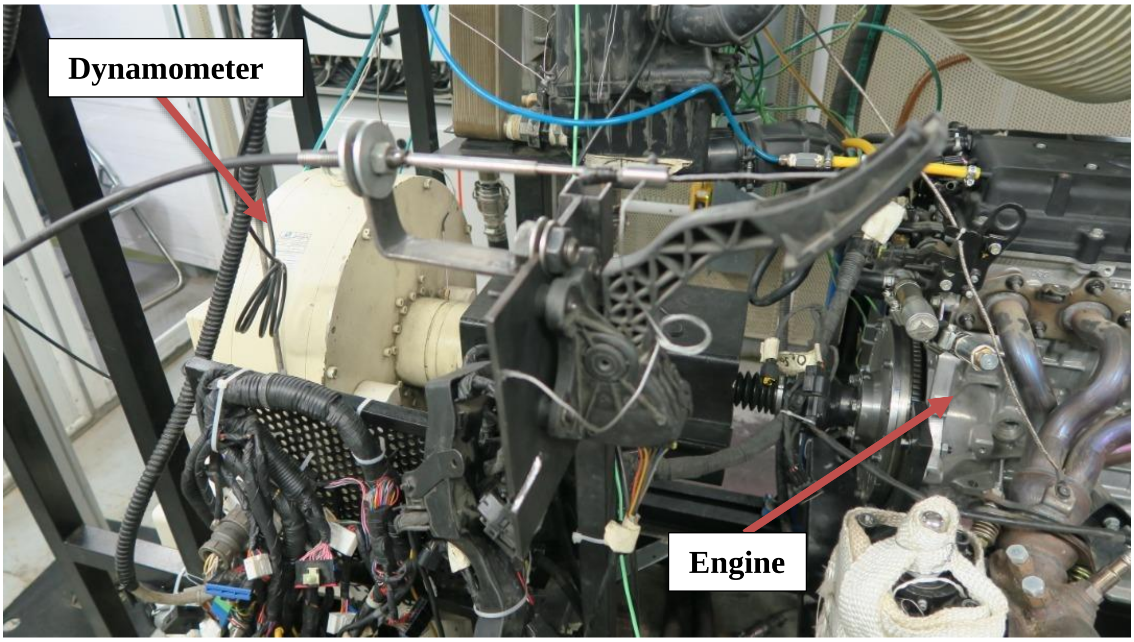

(b)

Fig.1 The KIA Cerato engine test bed

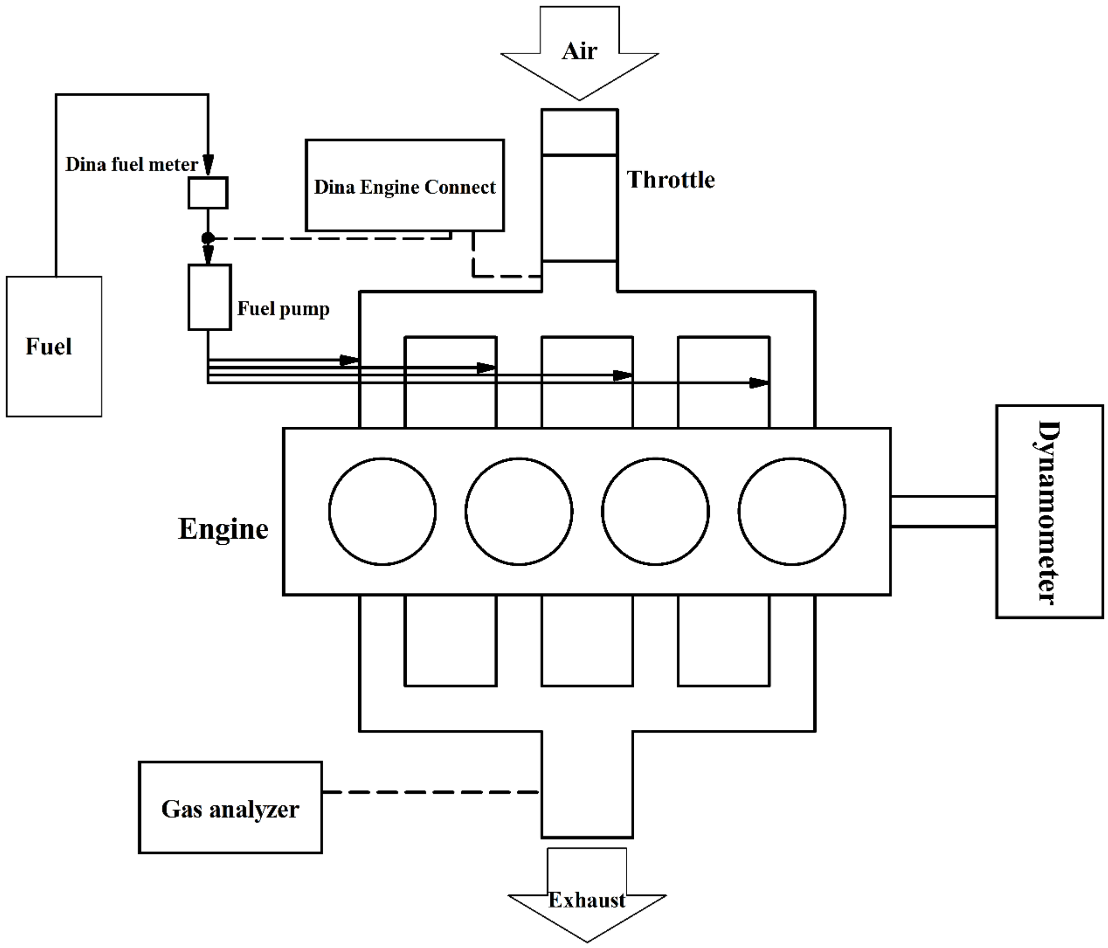

Fig.2 The KIA Cerato engine test bed schematic diagram

Table.2 Uncertainties of measuring instruments

Parameter	Unit	Measuring equipment	Nominal value range	Uncertainty	Relative uncertainty [%]
Air temperature	℃	Dina Engine Connect (38)	0-100	±2	2
Air pressure	kPa		0-100	±1	1
Relative humidity	%		5-95	±2.5	2.63
Fuel temperature	℃		0-100	±0.2	0.2
Engine speed	RPM	Schenck 190 kW Dynamometer (38)	100-7000	±4	5.71
Engine torque	Nm		0-250	±0.95	0.38
Engine power	kW		0-190	±1.2	0.63
NOx	ppm	Testo 350	0-4000	±10	0.25
Engine fuel consumption	kg/h	Dina Fuel Mass Flow Meter (38)	1-50	±0.25	0.5

2.2 Engine mathematical model

For developing the mathematical model of the KIA Cerato engine, AVL BOOST software was used. AVL BOOST is a 2D simulation software which performs highly accurate numerical analysis of the engines. It can deliver an advanced analysis for detailed prediction of engine performance and tailpipe emissions and it has been widely used by different researchers and automotive industries.

The block diagram of the model developed in AVL boost software are visualized in **Figure 3**. As shown, this engine configuration has 6 injectors (I1-I6). Injector 5 (I5) and 6 (I6) are employed for injection of hydrogen and water, respectively. After designing the block diagram of the proposed engine in the software, appropriate input parameters and mathematical models should be assigned to the model for enabling the software to provide the accurate output data using a set of complex algorithms. Formula Interpreter (FI1) block is used to calculate specific parameters such as the equivalent BSFC which are obtained by solving the external equations. Furthermore, water was injected into engine using single port injector as shown in Figure 3.

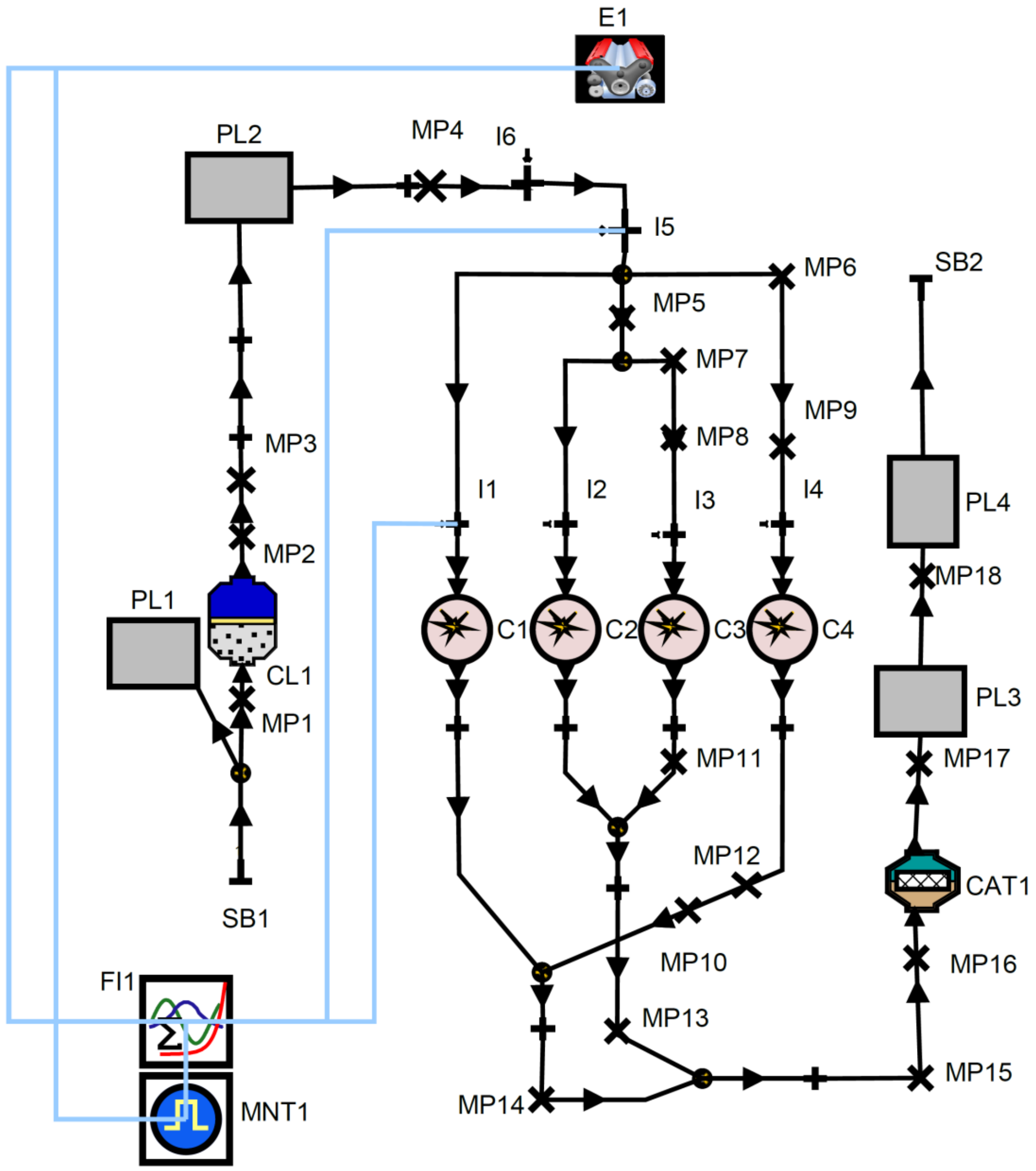

Fig.3 Block diagram of engine model in AVL BOOST software

2.2.1 Combustion model

The Vibe two-zone combustion model (15) is employed for mathematical modeling of the combustion process. This model is widely used in single and dual fuel engine systems for engine and emission analysis (39-46). The combustion chamber is divided into two zones, namely the *burned* and *unburned* zones. Therefore, this model can provide a meaningful prediction of unburnt hydrocarbon in unburned zones as well as the combustion. By applying first law of thermodynamic for each region the following equations are achieved (44):

$$\frac{dm_b u_b}{d\propto} = -P_c \frac{dV_b}{d\propto} + \frac{dQ_f}{d\propto} - \sum \frac{dQ_{wb}}{d\propto} + h_u \frac{dm_b}{d\propto} - h_{BB,b} \frac{dm_{BB,b}}{d\propto} \tag{1}$$

$$\frac{dm_u u_u}{d\propto} = -P_c \frac{dV_u}{d\propto} - \sum \frac{dQ_{wu}}{d\propto} - h_u \frac{dm_B}{d\propto} - h_{BB,u} \frac{dm_{BB,u}}{d\propto} \tag{2}$$

Where dm_u, $P_c \frac{dV_b}{d\propto}$, $\frac{dQ_f}{d\propto}$, $\frac{dQ_w}{d\propto}$, $h_u \frac{dm_b}{d\propto}$ and $h_{BB,b} \frac{dm_{BB,b}}{d\propto}$ terms are variation of in-cylinder internal energy, piston work, fuel input energy, wall heat losses, enthalpy flow from unburnt to burnt zone and blow by enthalpy, respectively. For volume changes of each zone, the equations can be expressed as follow (44):

$$\frac{dV}{d\propto} = \frac{dV_b}{d\propto} + \frac{dV_u}{d\propto} \tag{3}$$

$$V = V_b + V_u \tag{4}$$

In the Vibe two-zone model, the fuel mass burned fraction (*x*) during combustion is expressed as below (33, 44):

$$x = 1 - \exp\left[-a \left(\frac{\propto - SOC}{BDUR}\right)^{m+1}\right] \tag{5}$$

Here, *SOC*, *BDUR*, $\propto$, *m* and *a* are parameters representing the *start of the combustion, burn duration, crankshaft angle, Vibe shape* and *Vibe parameter*, consecutively. Vibe shape parameter indicates the position of the brunt for the combustion position. By employing such a combustion model with less complexity, large amount of time can be saved in simulation specially when the optimization is involved. However, the model should be precisely validated prior to any analysis. Vibe two-zone model has been used in previous related studies in the field (15, 47-49) and selected for this study as well, while a detailed validation process was performed.

2.2.2 Heat transfer model

The Woschni 1978 heat transfer model was used for modelling of the heat transfer between gas and cylinder walls (33, 44 , 50-52). This model accounts for the increase in the gas velocity in the cylinder during combustion and is superior to earlier models which generally assume a constant characteristic gas velocity equal to the mean piston speed. In Woschni 1978 in-cylinder heat transfer model, the heat transfer to the walls of the combustion chamber, i.e. the cylinder head, the piston, and the cylinder liner, is calculated from:

$$Q_{wi} = A_i \alpha_w (T_c - T_{wi}) \quad (6)$$

Where Q_{wi}, A_i, α_w, T_c and T_{wi} are wall heat flow, surface area, heat transfer coefficient, gas temperature in the cylinder and wall temperature, respectively. The α_w for the high-pressure cycle in Woschni 1978 model is summarized as follows (53):

$$\alpha_w = 130 D^{-0.2} p_c^{0.8} T_c^{-0.53} \left[C_1 c_m + C_2 \frac{V_D T_{c,1}}{p_{c,1} V_{c,1}} (p_c - p_{c,0}) \right]^{0.8} \quad (7)$$

$$C_1 = 2.28 + 0.308 \frac{c_u}{c_m} \quad (8)$$

D, c_u, c_m, V_D, $p_{c,0}$, $T_{c,1}$ and $p_{c,1}$ are cylinder bore, circumferential velocity, mean piston speed, displacement per cylinder, cylinder pressure of the motored engine, temperature in the cylinder at intake valve closing (IVC) and pressure in the cylinder at IVC, consecutively. C_2 equals to 0.00622 in this study because the engine used in this paper equipped with in-direct injection system. The Woschni 1978 model uses equation provided below for heat transfer coefficient in gas exchange process:

$$\alpha_w = 130D^{-0.2}p_c^{0.8}T_c^{-0.53}[C_3 c_m]^{0.8} \tag{9}$$

$$C_3 = 6.18 + 0.417\frac{c_u}{c_m} \tag{10}$$

2.2.3 Emission model

The Pattas and Hafner equation (33) combined with Zeldovich mechanism are employed for mathematical modeling of NOx formation rate in AVL BOOST as provided below (33):

$$r_{NO} = C_{PPM}C_{KM}(2,0)(1 - a_{NO}^2)\ [\frac{r_1}{1+a_{NO}AK_2} + \frac{r_4}{1+AK_4}] \tag{11}$$

$$a_{NO} = \frac{C_{NO.act}}{C_{NO.equ}}\frac{1}{C_{KM}} \tag{12}$$

$$AK_2 = \frac{r_1}{r_2+r_3} \tag{13}$$

$$AK_4 = \frac{r_4}{r_5+r_6} \tag{14}$$

Where C_{PPM}, C_{KM}, C_i and r_{NO} are post processing multiplier, kinetic multiplier, molar concentration and reaction rate of NOx, respectively. The equation provided by Onorati et al. (33) is used for modeling of CO formation:

$$r_{CO} = C_{cte}(r_1 - r_2)\,[1 - a_{CO}] \tag{15}$$

$$a_{CO} = \frac{c_{CO.act}}{c_{CO.equ}} \tag{16}$$

where r_{NO} and C_i are CO reaction rate and molar concentration, consecutively. Moreover, the complex phenomenological model for prediction of HC formation developed by AVL BOOST is employed for modeling of unburned hydrocarbons (HC) (33).

2.2.4 Fueling system parameters

In this study hydrogen has been injected to engine as secondary fuel, the lower heating value (LHV) of which is higher than that of gasoline fuel. Therefore, the equivalent BSFC has been computed using Eqn. (17) as presented below:

$$BSFC_{eqv} = \frac{\dot{m}_{gasoline} + \dot{m}_{H2}\frac{LHV_{H2}}{LHV_{gasoline}}}{\dot{W}_{engine}} \tag{17}$$

Here $\dot{m}_{gasoline}$, $\dot{m}_{H2}$ and $\dot{W}_{engine}$are the gasoline mass flow rate, hydrogen mass flow rate and engine power output parameters, respectively.

The hydrogen is injected into the engine at different energy shares. The hydrogen energy share shows the fraction of energy supplied by hydrogen instead of using gasoline fuel. The mass flow rates of hydrogen and gasoline fuels in various hydrogen energy shares are presented in **Table 3**. The *mass flow rate of hydrogen injection* in various engine conditions can be expressed as:

$$\dot{m}_{H2} = \dot{m}_{total\,fuel}\, mf_{H2}\frac{LHV_{gasoline}}{LHV_{H2}} \tag{18}$$

In Eqn. (18) $\dot{m}_{total\ fuel}$ and mf_{H2} are the total mass flow rate of fuel and hydrogen energy share, respectively. In addition, water is injected into engine at different engine speeds with different water-to-fuel ratios:

$$\dot{m}_{water} = \dot{m}_{total\ fuel}\, WIR \tag{19}$$

Where WIR and $\dot{m}_{water}$ designate the water-to-total fuel ratio and water mass flow rate, respectively. The water injection ratio is calculated using Eqn. (20):

$$WIR = \dot{m}_{water} / \dot{m}_{total\ fuel} \tag{20}$$

Table.3 Specifications of KIA Cerato engine

Hydrogen energy share	Gasoline mass flow rate [g/s]	Hydrogen mass flow rate [g/s]
0	8.47	0
0.05	8.058	0.149
0.1	7.649	0.288
0.2	6.866	0.537
0.3	6.123	0.748

2.3 Design of experiments analysis

Having an increasing number of parameters, the optimization process is going to be complex for this study. By employing the Design of Experiment (DoE) Methods, an optimized number of parameters can be generated in design space to run an efficient optimization process. In order to perform a parametric analysis for investigating the effects of injecting hydrogen and water into the engine, the Latin Hypercube DOE (design of experiments) method was used (54-57). In Latin Hypercube DOE method, random design points are generated in a multi-dimensional distribution. In this study, hydrogen energy share, water injection ratio and SOC were chosen as the design parameters in DOE method. The distribution of design points in the Latin Hypercube is shown in **Figure 4**. Each axis of Latin hypercube in **Figure 4**, belongs to the one of the design parameters defined for this study and the maximum and minimum values for each of the design parameters are also presented in **Table 4**.

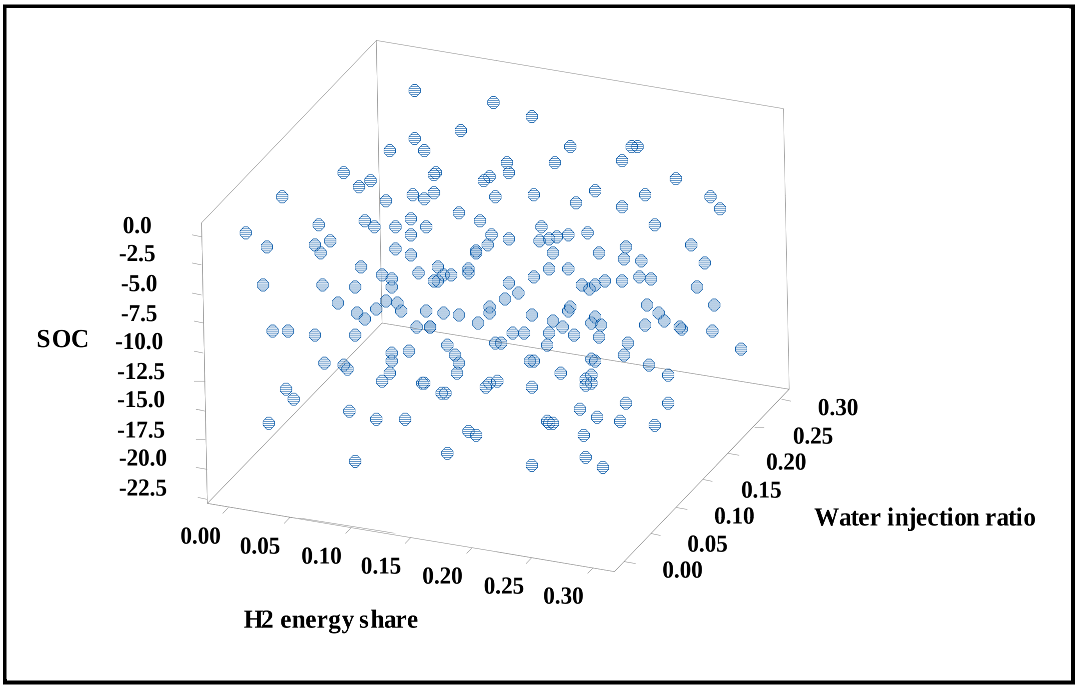

Fig.4 The sampling space and the design points in Latin Hypercube DOE method

Table.4 Maximum and minimum values of each design parameter

Parameter	Unit	Minimum value	Maximum value
H2 energy share	-	0	0.3
Water injection ratio	-	0	0.3
SOC	Degree	-20	0

There are 200 design points in sampling space of the Latin Hypercube. Therefore, each response will be calculated for all 200 points in the sampling space for this study. Following this, the regression will be employed to obtain relationships between responses and design parameters which lead to the *optimization* phase.

2.4 Multi-objective optimization

As mentioned in previous section, the relation between each of the responses and design parameters were obtained by using regression analysis. The equation obtained from regression analysis are used for multi-objective optimization using genetic algorithm (GA) method (58, 59). The optimization criteria are provided in **Table 5**. There is a trade-of between the selected two objective functions (BMEP and NOx_{MFR}) for selected design parameters (hydrogen energy share, water injection ratio and SOC), that's why multi-objective optimization was performed using MATLAB software. The pareto front diagrams showing the optimum point for each hydrogen energy share were obtained during optimization. Then, the ideal point in each pareto front diagram indicating the optimum point for each hydrogen energy share was identified.

Table.5 The optimization criteria

Objective	Criterion	Minimum value	Maximum value
BMEP [bar]	Max	8.84	10.04
$\boldsymbol{NOx_{MFR}}$ [kg/s]	Min	25e-6	55e-6

The principal targets of multi-objective optimization are *maximizing BMEP* (minimizing -BMEP) and *minimizing NOx* emissions. Figure 5 presents the procedure in which the experiments, mathematical modelling and optimization process were performed

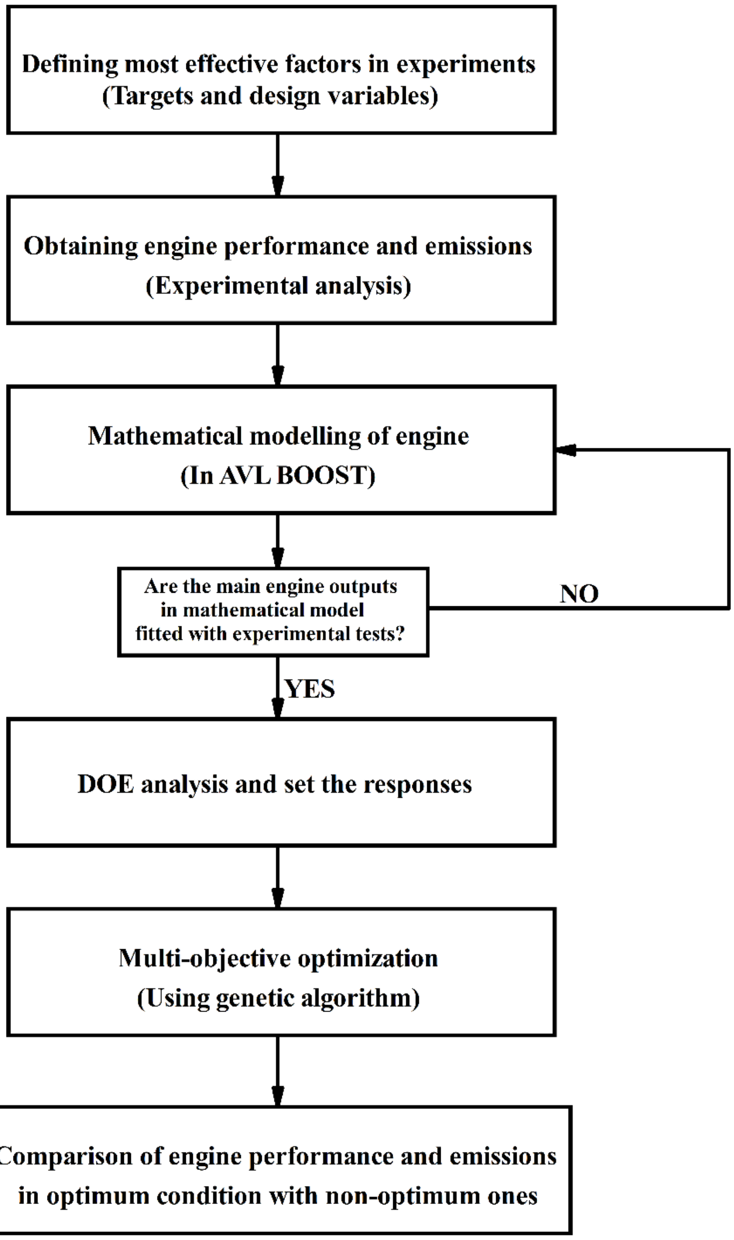

Fig.5 The flow chart of experiments and optimization process in this study

3. Validation

For validation of the AVL model, the BSFC, engine torque output and NOx have been compared with experimental results. The experiments were conducted precisely using a specialized testbed and the required results were extracted for validation. The results of the comparison are illustrated in **Table 6**. Inspection of this table demonstrates that the model is in good agreement with the experimental data for different conditions. As can be seen, the errors are higher in low RPMs compared to high RPMs as the result of the less stability of the engine at lower RPMs. Furthermore, the maximum error arising from the comparison of data between the experiments and the AVL model is below 8%. Therefore, the validity of the model is confirmed, and it is applied with justifiable confidence in the rest of this investigation.

Table.6 Comparison of engine torque, BSFC and NOx production rate of AVL model with experimental tests in different RPMs

Engine speed (RPM)	Engine torque [Nm]			Engine BSFC [g/kWh]			NOx production rate [ppm]		
	AVL model	Experiment	Error [%]	AVL model	Experiment	Error [%]	AVL model	Experiment	Error [%]
1000	137.1	148.1	7.434	299	306.5	2.44	478	444	7.65
2000	152.8	161.9	5.627	275.1	294.9	6.721	804	843	4.62
4000	185.4	191.7	3.312	284.7	273.3	4.157	672	650	3.38
6000	151.9	153.1	0.7838	319.9	319.8	0.024	558	540	3.3
6500	136.9	140.2	2.375	337.3	342	1.387	439	456	3.72
7000	123.9	129.8	4.569	352.2	358	1.611	413	402	2.73

4. Result and discussion

4.1 Regression and variance analysis

The regression analysis was performed to define the relationship between the objective functions (BMEP and NOx) and design parameters (H2 energy share, WIR and SOC) for the multi-objective genetic algorithm (GA) optimization. Two selected objective functions (called "Responses") are presented in **Table 7** and are defined based on the design parameters elucidated in Eqn. (21) as follows:

$$Response = cte + a.SOC + b.H2_{ES} + c.WIR + d.SOC.H2_{ES} + e.SOC.WIR + f.H2_{ES}.WIR + g.SOC^2 + h.H2_{ES}{}^2 + i.WIR^2 \quad (21)$$

The constant parameters and multipliers of Eqn. (21) are presented in **Table 7** for each of the objective functions (Responses) at the rated condition (6000 RPM). The fitting goodness analysis for each Response (BMEP and NOx) has also been performed and the results are provided in **Table 8**. As shown, the *maximum error of regression fitting* is below 1% which is a strong verification of the high precision achieved with the current mathematical model.

Table.7 The regression constant parameters and multipliers

Responses	***cte***	***a***	***b***	***c***	***d***	***e***	***f***	***g***	***h***	***i***
BMEP	8.971	-0.109	-2.412	3.653	-0.0096	-0.0067	4.469	-0.0038	0.0896	-5.699
Indicated Efficiency (IE)	0.339	-0.003	0.144	-0.25	-0.001	0.0009	-0.211	-0.0001	0.113	0.099
PCT	2501.52	-5.35	-99.84	82.22	-3.48	1.97	468.01	0.214	49.36	-789.41
NOx production	3.581e-5	-3.409e-6	-9.141e-5	2.883e-5	4.503e-6	-2.313e-6	0.0003	2.769e-8	2.785e-5	0.00035
HC production	3.566e-5	-7.876e-7	-2.590e-5	3.17e-5	3.914e-7	-6.864e-7	-1.238e-6	1.459e-9	2.152e-6	-3.703e-6
CO production	0.006	2.828e-5	-0.0005	-0.0032	-2.763e-5	-6.519e-6	-0.0018	5.504e-7	-0.0049	0.00066

Table.8 The fitness analysis of regression

Responses	P-value	R^2
BMEP	<0.0001	0.99
IE	<0.0001	0.99
PCT	<0.0001	0.99
NOx production	<0.0001	0.99
HC production	<0.0001	0.99
CO production	<0.0001	0.99

4.2 Multi-objective optimization

The equations developed by regression analysis in the previous section were used in the optimization process. As elaborated in the literature review, hydrogen injection will result in power reduction in engines (15, 19). On the other hand, any attempt to compensate this power reduction, would increase the NOx production (12), and a trade-off, therefore, exists. In accordance with the constraints, BMEP and NOx production rate have been considered as the objective functions for the optimization process. The optimization is performed to determine as accurately as possible, the optimum values of WIR, SOC for each hydrogen energy shares.

Figure 6 presents the Pareto frontier for one of the hydrogen energy shares. As shown, a clear trade-off between 2 objective functions are observed. The nearest point (optimum design point) to the ideal point is also identified. The behaviors for other energy shares were the same and all of the optimum design points (nearest point to ideal point) for each hydrogen shares are summarized in **Table 9**.

Based on the results provided in **Table 9**, water should be injected at the maximum rate to optimize the engine while the optimum values of SOC angle vary in the range between -6.23 and -2.65 for various hydrogen energy shares.

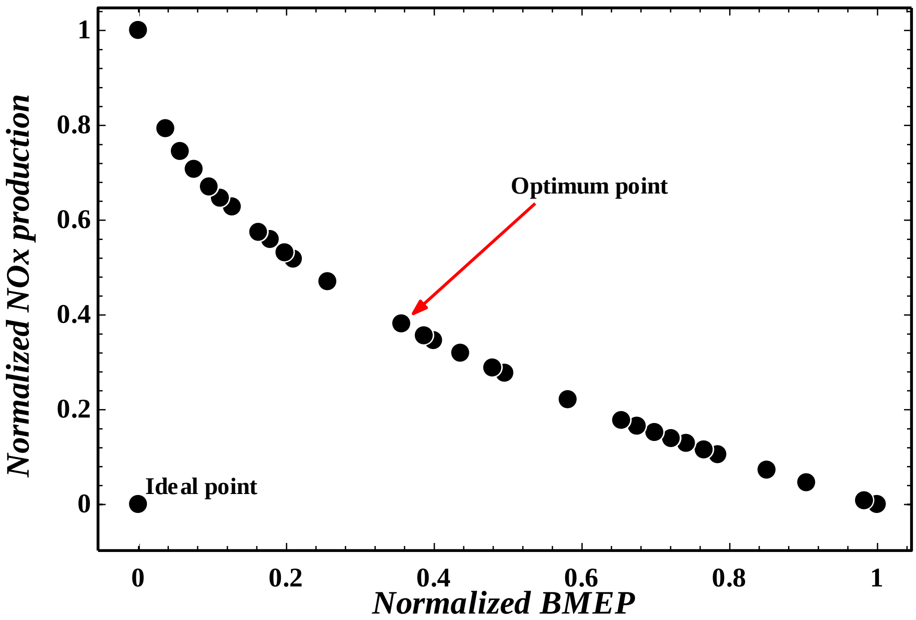

Fig.6 The Pareto optimal frontier for the H2 energy share of 0.05

Table.9 The optimum design point specifications for various hydrogen energy shares

Hydrogen energy share	Optimized values	
	Water injection ratio	Start of combustion (SOC) [deg]
0.05	0.3	-5.9
0.1	0.3	-5.19
0.2	0.3	-6.23
0.3	0.3	-2.65

4.2 Parametric analysis and comparison

To further develop the analysis, *four optimum designed points* obtained in the previous section were used in the model to study the engine performance in different scenarios. The comparison was made to investigate the benefits of optimized water injection and SOC on various engine performance parameters. The results of optimized co-injection were compared to the single fueled gasoline engine (same engine without hydrogen and water injection) and with the hydrogen dual fueled engine without any water injection and SOC modification.

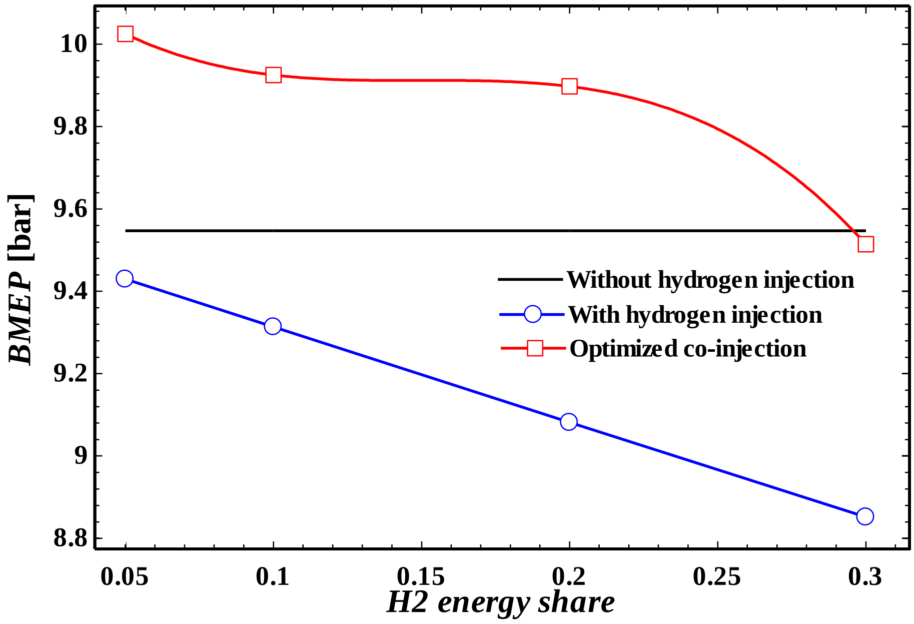

Fig.7 The engine BMEP for various hydrogen energy shares with different fueling modes

Figure 7 shows the BMEP trend by hydrogen injection for various hydrogen energy shares. As can be seen, injection of hydrogen to the engine reduces the engine BMEP compared to the original engine operating purely on gasoline fuel. The reduction in BMEP is between 1.36% to 7.33% with the *highest reduction corresponding to the highest hydrogen injection* which is mainly attributable to the reduction of engine volumetric efficiency, as also reported by Magryta *et al*. (15). However, the optimized injection of water with SOC modification clearly exerts a positive effect and recovers the engine BMEP; additionally, an increase of 8.8% in BMEP is observed at 5% hydrogen energy share. Therefore, the SOC modification with optimized injection of water has been shown to not only completely compensate the BMEP drop caused by hydrogen injection into the engine, but to achieve a supplementary boost in BMEP value.

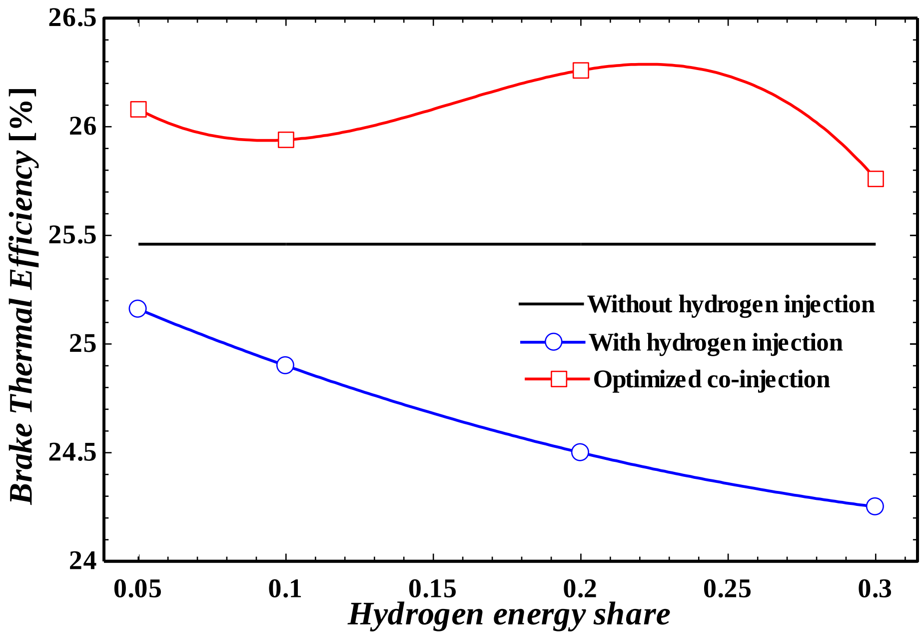

Fig.8 The engine brake thermal efficiency for various hydrogen energy shares with different fuel modes

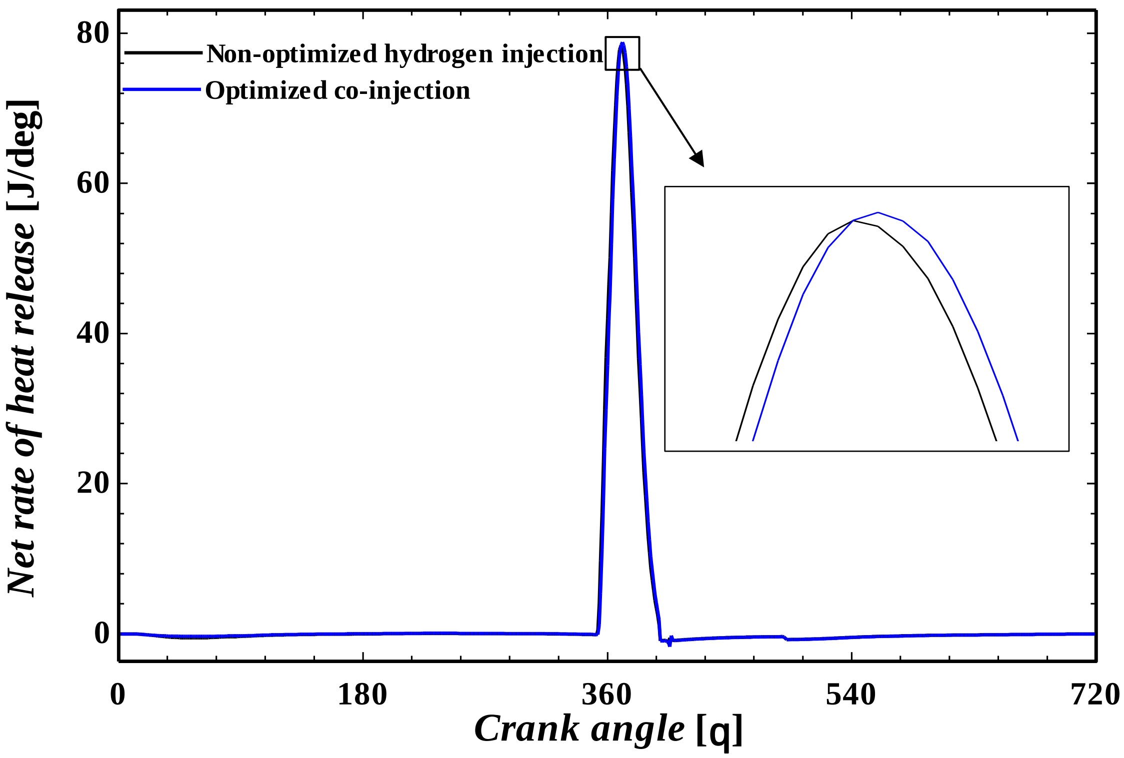

Fig.9 The net rate of heat release at various crank angles at hydrogen energy share of 0.2

The variation of engine brake thermal efficiency at various hydrogen shares is shown in **Figure 8**. According to the results, injection of hydrogen without any modification results in reduction of engine brake thermal efficiency between 0.3% and 1.2% for various hydrogen energy shares. On the other hand, by injection of water and modification of SOC with optimum values, the engine brake thermal efficiency is distinctly improved when compared to the single fueled engine for different hydrogen energy shares. The impact of optimization of SOC and water injection rate on the net rate of heat release at hydrogen energy share of 0.2 is presented in **Figure 9**. As can be seen, the peak value of heat release is slightly higher for optimal case, and the it is shifted to the right. This increment of rate of heat release resulted by optimal injection of water and modification of SOC has reflected on increase of engine BMEP and brake thermal efficiency as presented in **Figures 7 and 8**.

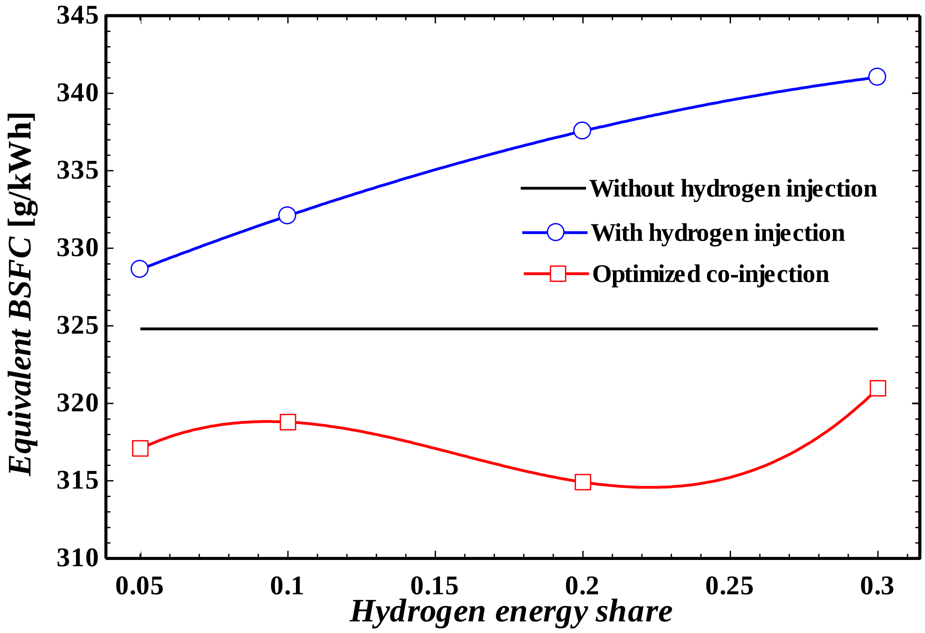

Fig.10 The engine equivalent BSFC at various hydrogen energy shares with different fuel modes

The effects of hydrogen injection on BSFC for different fueling modes are presented in **Figure 10**. The engine equivalent BSFC is enhanced via injection of hydrogen at various hydrogen shares up to 4.61% in comparison to the condition where engine is fueled by gasoline due to the engine power reduction (as a result of the decrease in BMEP). However, by simultaneous optimization of the water injection and SOC, the engine equivalent BSFC is decreased between 1.23% and 3% compared to the original condition for different H_2 energy shares. This confirms the positive effect of the adopted optimization approach on fuel consumption for hydrogen addition into the fuel.

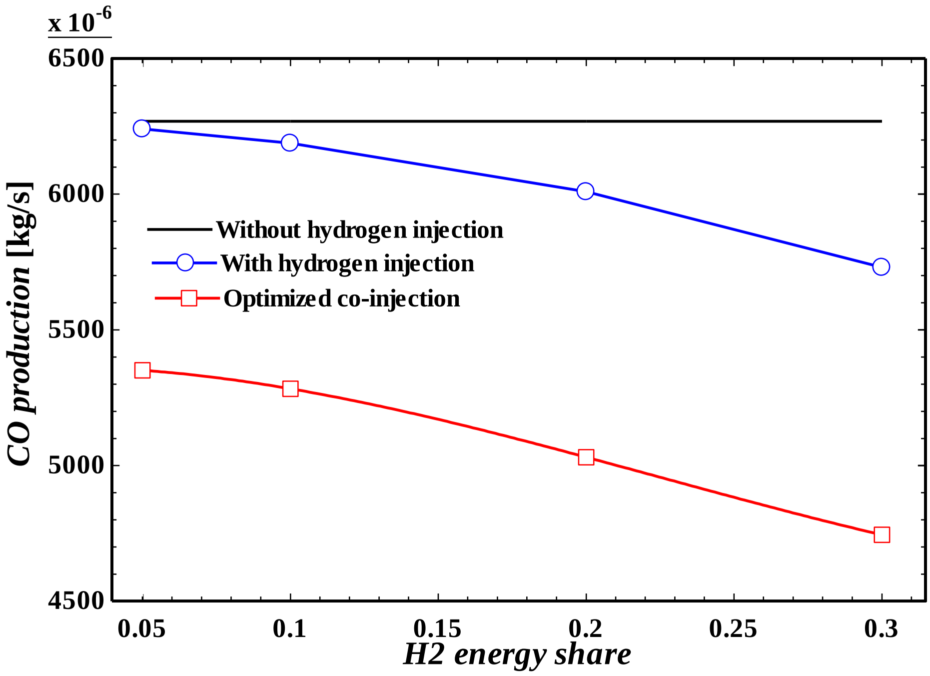

Fig.11 The engine CO production rate at various hydrogen energy shares with different fuel modes

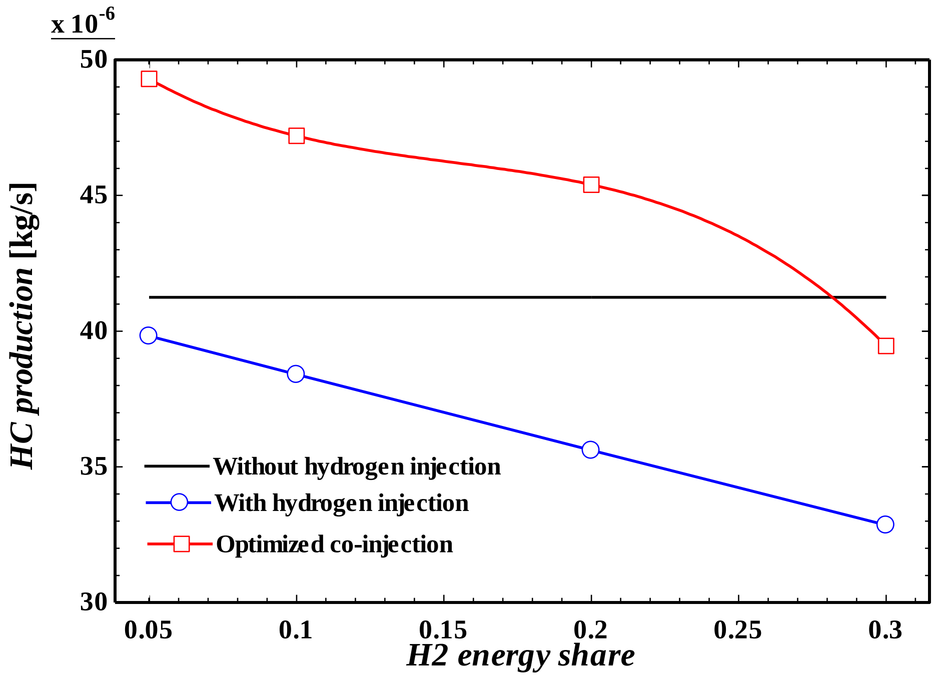

Fig.12 The engine HC production rate at various hydrogen energy shares for different fuel modes

The effects of H_2 injection on CO and HC emissions are presented in **Figures 11 and 12**. As indicated, the CO production decreases continuously by injection of hydrogen up to 8.8%, whereas optimized co-injection of water results in a significant reduction of about 25% compared to the original condition (due to the improvement of combustion performance by injection of water and modification of SOC angle with optimum values). However, the trend for HC is not the same. While hydrogen injection caused a continuous reduction in HC emissions between 2.4% to 19.5% compared to original condition, optimized injection produces an increase in engine HC production from the hydrogen shares of between 5%-20%. Since Hydrogen is not a hydrocarbon fuel and the hydrogen molecules do not contain any carbon, increment of hydrogen mass fractions in the fuel results in reduction of HC production rate. On the other hand, injection of water into the engine results in reduction of the in-cylinder mixture temperature. This reduction in temperature leads to increase of unburnt local zones inside the cylinder resulting in increase of HC production rate. Increase in HC production rate could be caused by the *moderate increase of unburnt zones* in the combustion chamber induced by virtue of an increase of water content in the combustion chamber. Only when the hydrogen share reaches 30% does the engine HC level drop below the gasoline fueled engine.

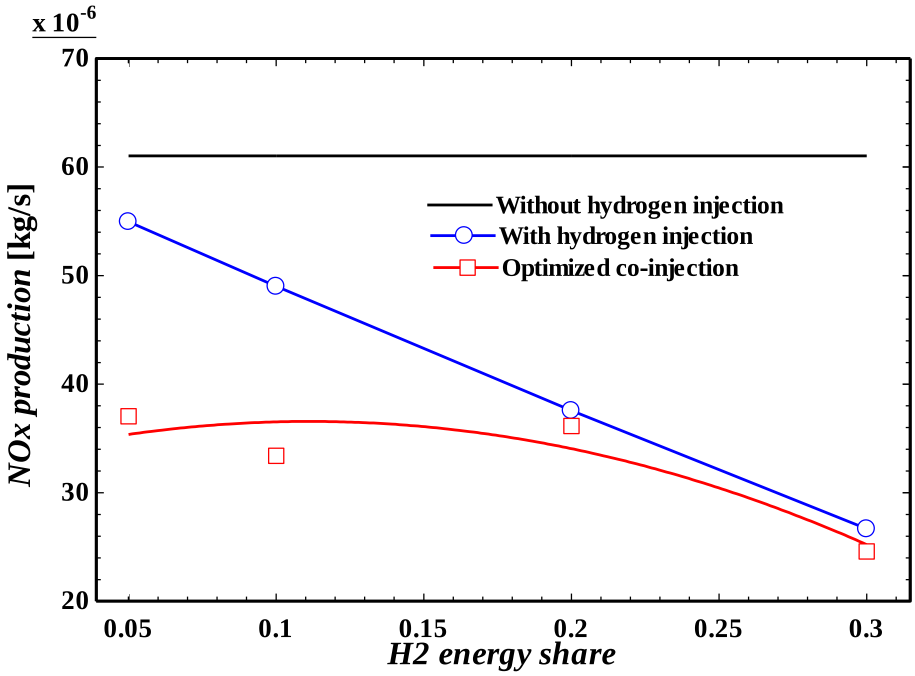

Fig.13 The engine NOx production rate at various hydrogen energy shares for different fuel modes

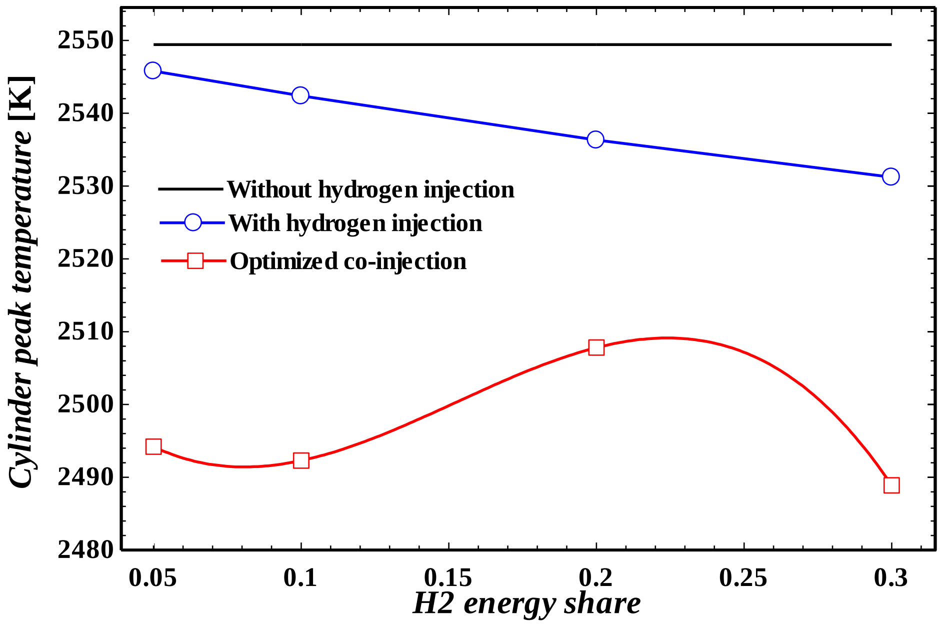

Fig.14 The cylinder peak temperature at various hydrogen energy shares for different fuel modes

The engine NOx emission rate at various hydrogen shares for different fueling modes are displayed in **Figure 13**. NOx production rate is decreased by hydrogen injection for both optimized and unoptimized scenarios. However, optimized co-injection of water and SOC modification influence engine performance more positively in terms of NOx reduction and a significant NOx reduction (up to nearly 59%) is achieved. The reduction in NOx could be relevant to *in-cylinder temperature decrease* when water is injected as shown in **Figure 14**. NOx reduction trend was reported by Ji *et al.* (19) in the literature. The other reason is the reduction of engine volumetric efficiency which results in *engine torque and cylinder pressure reduction* by injection of hydrogen at various energy shares (15) when air-to-fuel ratio is fixed. The results for NOx reduction correlate closely with experimental work in literature and follow a similar trend for NOx reduction in spark ignition engines to that reported by Ji *et al*. (19).

5.Conclusions

In this research, a 4-cylinder gasoline engine was optimized for hydrogen injection as the secondary fuel using AVL software. This study has addressed the power loss in hydrogen/gasoline dual fueled engines with a novel and innovative approach. The effect of water injection, SOC modification and hydrogen injection at different energy shares on the performance of a hydrogen/gasoline dual fueled engine, has been investigated. The hydrogen has been injected into the engine at different energy shares. The main results drawn from this study may be summarized as follows:

- Optimized co-injection of water with start of combustion (SOC) modification in various hydrogen energy shares achieves good compensation of the power drop due to hydrogen injection as indicated by BMEP.
- Injection of hydrogen without any modification results in a reduction in engine brake thermal efficiency between 0.3% and 1.2% for various hydrogen energy shares. However, by injection of water and modification of SOC with optimum values, the engine brake thermal efficiency is successfully increased due to the increase of heat release rate even above the original single fueled engine.
- The peak of net rate of heat release is increased by optimum co-injection of water and hydrogen compared to hydrogen/gasoline dual fueling mode without water injection and SOC modification.
- The engine equivalent BSFC considerably increases by injection of hydrogen at various energy shares; however, with optimized co-injection of water and hydrogen, the engine equivalent BSFC decreases to between 1.23% and 3% compared to the original condition.
- By water injection into the engine, the total temperature of the in-cylinder gas mixture decreases, indicating that the engine NOx rate has dropped below the rate of single fuel and dual fueled engines without modification.
- Optimized simultaneous injection of water and hydrogen into the engine results in a CO reduction rate of about 25% compared to the single and dual fueled mode; however, the HC production rate increases relative to other fueling modes at various hydrogen energy shares caused by the moderate increase of unburnt zones in the engine combustion chamber by water injection.
- The results of this work have demonstrated the benefits of adding water to hydrogen/gasoline dual fuel engine and SOC tuning for compensating the power

loss caused by hydrogen injection at various energy shares as well as the NOx reduction. It can be a valuable reference for automotive industry for future testing of the proposed solutions in real practice.

- The results of this study confirm the need for further modifications and the optimization approach in designing 21st century hydrogen injection mechanisms for hydrogen/gasoline dual fueled engines. The study of temperature variation of injected water into the engine is suggested for future research. Furthermore, more complex combustion model such as fractal can be considered instead of the Vibe two-zone model in future works.

Nomenclature		
a	Vibe parameter	
BMEP	Brake mean effective pressure	
BSFC	Brake specific fuel consumption	
BDUR	Burn duration	
C	Cylinder	
CAT	Catalytic converter	
CL	Air cleaner	
cte	Constant parameter	
E	Engine	
ED	Electrical generator	
EV	Electric vehicle	
FCHEV	Fuel cell hybrid electric vehicle	
HEV	Hybrid electric vehicle	
IC engine	Internal combustion engine	
LHV	Lower Heating Value	
m	Vibe shape	
MC	Mechanical connection	
MP	Measuring point	
PCT	Peak cylinder temperature	
PL	Plenum	
SB	System boundary	
SOC	Start of combustion	
WIR	Water injection ratio	
$\propto$	Crank shaft angle	
Subscripts		
ES	Energy share	

6.Acknowledgement

AVL List GmbH support for proving the simulation tools for University of Salford through their University Partnership Program is greatly appreciated. Special thanks to Dina Motors company for their support during this research.

References

1. Salek F, Moghaddam AN, Naserian MM. Thermodynamic analysis of diesel engine coupled with ORC and absorption refrigeration cycle. Energy Conversion and Management. 2017;140:240-6.
2. Salek F, Babaie M, Ghodsi A, Hosseini SV, Zare A. Energy and exergy analysis of a novel turbo-compounding system for supercharging and mild hybridization of a gasoline engine. Journal of Thermal Analysis and Calorimetry. 2020:1-12.
3. Wang L, Collins EG, Li H. Optimal design and real-time control for energy management in electric vehicles. IEEE Transactions on Vehicular Technology. 2011;60(4):1419-29.
4. Ji C, Yang J, Liu X, Wang S, Zhang B, Wang D. Enhancing the fuel economy and emissions performance of a gasoline engine-powered vehicle with idle elimination and hydrogen start. Applied energy. 2016;182:135-44.
5. Yu X, Wu H, Du Y, Tang Y, Liu L, Niu R. Research on cycle-by-cycle variations of an SI engine with hydrogen direct injection under lean burn conditions. Applied Thermal Engineering. 2016;109:569-81.
6. Mandel S. Green hydrogen and the future of sustainable energy use in South Africa. AIP Publishing LLC; 2019.
7. Singh S, Jain S, Venkateswaran P, Tiwari AK, Nouni MR, Pandey JK, et al. Hydrogen: A sustainable fuel for future of the transport sector. Renewable and Sustainable Energy Reviews. 2015;51:623-33.
8. Ji C, Wang S, Zhang B, Liu X. Emissions performance of a hybrid hydrogen–gasoline engine-powered passenger car under the New European Driving Cycle. Fuel. 2013;106:873-5.
9. Salek F, Zamen M, Hosseini SV. Experimental study, energy assessment and improvement of hydroxy generator coupled with a gasoline engine. Energy Reports. 2020;6:146-56.
10. Salek F, Zamen M, Hosseini SV, Babaie M. Novel hybrid system of pulsed HHO generator/TEG waste heat recovery for CO reduction of a gasoline engine. International Journal of Hydrogen Energy. 2020;45(43):23576-86.
11. Zhou J, Guo Y, Huang Z, Wang C. A review and prospects of gas mixture containing hydrogen as vehicle fuel in China. International Journal of Hydrogen Energy. 2019;44(56):29776-84.
12. Kim J, Chun KM, Song S, Baek H-K, Lee SW. Hydrogen effects on the combustion stability, performance and emissions of a turbo gasoline direct injection engine in various air/fuel ratios. Applied Energy. 2018;228:1353-61.
13. Li G, Yu X, Jin Z, Shang Z, Li D, Li Y, et al. Study on effects of split injection proportion on hydrogen mixture distribution, combustion and emissions of a gasoline/hydrogen SI engine with split hydrogen direct injection under lean burn condition. Fuel. 2020;270:117488.
14. Yu X, Du Y, Sun P, Liu L, Wu H, Zuo X. Effects of hydrogen direct injection strategy on characteristics of lean-burn hydrogen–gasoline engines. Fuel. 2017;208:602-11.

15. Magryta P, Wendeker M, Majczak A, Bialy M, Siadkowska K. Simulation Studies of SI Engine that Meets the Euro5 Standard, Supply by Gasoline with the Hydrogen Addition. SAE Technical Paper; 2014. Report No.: 0148-7191.
16. Wang S, Ji C, Zhang B, Liu X. Lean burn performance of a hydrogen-blended gasoline engine at the wide open throttle condition. Applied energy. 2014;136:43-50.
17. Faizal M, Chuah L, Lee C, Hameed A, Lee J, Shankar M. Review of hydrogen fuel for internal combustion engines. Journal of Mechanical Engineering Research and Developments. 2019;42(3):35-46.
18. Gęca M, Litak G. Mean effective pressure oscillations in an IC-SI engine after the addition of hydrogen-rich gas. Measurement. 2017;108:18-25.
19. Ji C, Wang S. Effect of hydrogen addition on the idle performance of a spark ignited gasoline engine at stoichiometric condition. International journal of hydrogen Energy. 2009;34(8):3546-56.
20. Chen B, Zhang L, Han J, Chen X. Investigating the effect of increasing specific heat and the influence of charge cooling of water injection in a TGDI engine. Applied Thermal Engineering. 2019;149:1105-13.
21. Elsemary IM, Attia AA, Elnagar KH, Elsaleh MS. Spark timing effect on performance of gasoline engine fueled with mixture of hydrogen–gasoline. International Journal of Hydrogen Energy. 2017;42(52):30813-20.
22. Wang J, Duan X, Liu Y, Wang W, Liu J, Lai M-C, et al. Numerical investigation of water injection quantity and water injection timing on the thermodynamics, combustion and emissions in a hydrogen enriched lean-burn natural gas SI engine. International Journal of Hydrogen Energy. 2020.
23. Xu P, Ji C, Wang S, Cong X, Ma Z, Tang C, et al. Effects of direct water injection on engine performance in engine fueled with hydrogen at varied excess air ratios and spark timing. Fuel. 2020;269:117209.
24. Li A, Zheng Z, Peng T. Effect of water injection on the knock, combustion, and emissions of a direct injection gasoline engine. Fuel. 2020;268:117376.
25. Elsemary IM, Attia AA, Elnagar KH, Elaraqy AA. Experimental investigation on performance of single cylinder spark ignition engine fueled with hydrogen-gasoline mixture. Applied Thermal Engineering. 2016;106:850-4.
26. Venugopal T, Ramesh A. Effective utilisation of butanol along with gasoline in a spark ignition engine through a dual injection system. Applied thermal engineering. 2013;59(1-2):550-8.
27. Ji C, Yan H, Wang S. Simulation Study on Combustion Characteristics of a Spark Ignition Engine Fueled with Gasoline—Hydrogen Fuel Mixture. SAE Technical Paper; 2009. Report No.: 0148-7191.
28. Dhyani V, Subramanian K. Control of backfire and NOx emission reduction in a hydrogen fueled multi-cylinder spark ignition engine using cooled EGR and water injection strategies. International Journal of Hydrogen Energy. 2019;44(12):6287-98.
29. Chintala V, Subramanian K. Hydrogen energy share improvement along with NOx (oxides of nitrogen) emission reduction in a hydrogen dual-fuel compression ignition engine using water injection. Energy conversion and management. 2014;83:249-59.
30. Gürbüz H. Analysis of the effects of multiple injection strategies with hydrogen on engine performance and emissions in diesel engine. International Journal of Hydrogen Energy. 2020;45(51):27969-78.
31. Arat HT. Alternative fuelled hybrid electric vehicle (AF-HEV) with hydrogen enriched internal combustion engine. International Journal of Hydrogen Energy. 2019;44(34):19005-16.
32. Juknelevičius R, Rimkus A, Pukalskas S, Matijošius J. Research of performance and emission indicators of the compression-ignition engine powered by hydrogen-Diesel mixtures. International Journal of Hydrogen Energy. 2019;44(20):10129-38.

33. Salek F, Babaie M, Redel-Macias MD, Ghodsi A, Hosseini SV, Nourian A, et al. The effects of port water injection on spark ignition engine performance and emissions fueled by pure gasoline, E5 and E10. Processes. 2020;8(10):1214.
34. Atmanli A, Ileri E, Yilmaz N. Optimization of diesel–butanol–vegetable oil blend ratios based on engine operating parameters. Energy. 2016;96:569-80.
35. Yilmaz N, Ileri E, Atmanlı A, Deniz Karaoglan A, Okkan U, Sureyya Kocak M. Predicting the engine performance and exhaust emissions of a diesel engine fueled with hazelnut oil methyl ester: the performance comparison of response surface methodology and LSSVM. Journal of Energy Resources Technology. 2016;138(5).
36. Ileri E, Karaoglan AD, Atmanli A. Response surface methodology based prediction of engine performance and exhaust emissions of a diesel engine fuelled with canola oil methyl ester. Journal of Renewable and Sustainable Energy. 2013;5(3):033132.
37. Verhelst S, Maesschalck P, Rombaut N, Sierens R. Efficiency comparison between hydrogen and gasoline, on a bi-fuel hydrogen/gasoline engine. International journal of hydrogen energy. 2009;34(5):2504-10.
38. Dinamotors Company [Available from: www.dinamotors.com.
39. Banday S, Wani MM. Computational parametric investigations on a single cylinder spark ignition engine using ethanol-gasoline blends for power generation. International Journal of Mechanical Engineering and Robotics Research. 2015;4(2):105.
40. Iliev SP, editor Developing of a 1-D combustion model and study of engine characteristics using ethanol-gasoline blends. Proceedings of the World Congress on Engineering; 2014.
41. Xiang L, Song E, Ding Y. A Two-Zone Combustion Model for Knocking Prediction of Marine Natural Gas SI Engines. Energies. 2018;11(3):561.
42. Pešić RB, Davinić AL, Taranović DS, Miloradović DM, Petković SD. Experimental determination of double vibe function parameters in diesel engines with biodiesel. Thermal science. 2010;14(suppl.):197-208.
43. Verhelst S, Sheppard C. Multi-zone thermodynamic modelling of spark-ignition engine combustion–an overview. Energy Conversion and management. 2009;50(5):1326-35.
44. Iliev S. A comparison of ethanol and methanol blending with gasoline using a 1-D engine model. Procedia Engineering. 2015;100:1013-22.
45. Baškovič UŽ, Katrašnik T. Real-time capable virtual NOx sensor for diesel engines based on a two-Zone thermodynamic model. Oil & Gas Sciences and Technology–Revue d'IFP Energies nouvelles. 2018;73:11.
46. Zhang Z, Jiaqiang E, Chen J, Zhao X, Zhang B, Deng Y, et al. Effects of boiling heat transfer on the performance enhancement of a medium speed diesel engine fueled with diesel and rapeseed methyl ester. Applied Thermal Engineering. 2020;169:114984.
47. Gürbüz H. Analysis of the effects of multiple injection strategies with hydrogen on engine performance and emissions in diesel engine. International Journal of Hydrogen Energy. 2020.
48. Karagöz Y, Balcı Ö, Köten H. Investigation of hydrogen usage on combustion characteristics and emissions of a spark ignition engine. International Journal of Hydrogen Energy. 2019;44(27):14243-56.
49. Ayad SM, Belchior CR, da Silva GL, Lucena RS, Carreira ES, de Miranda PE. Analysis of performance parameters of an ethanol fueled spark ignition engine operating with hydrogen enrichment. International Journal of Hydrogen Energy. 2020;45(8):5588-606.
50. Ogink R, Golovitchev V. Gasoline HCCI modeling: Computer program combining detailed chemistry and gas exchange processes. SAE Transactions. 2001:2338-50.
51. Kitanoski F, Puntigam W, Kozek M, Hager J. An engine heat transfer model for comprehensive thermal simulations. SAE Technical Paper; 2006. Report No.: 0148-7191.

52. Ping Z, Guangyao O, Lufeng B, editors. Simulation on thermal performance parameters of gas-fired in cylinder based on Boost software. 2010 International Conference on Computer, Mechatronics, Control and Electronic Engineering; 2010: IEEE.

53. Woschni G. A universally applicable equation for the instantaneous heat transfer coefficient in the internal combustion engine. SAE transactions. 1968:3065-83.

54. Viana FA, Venter G, Balabanov V. An algorithm for fast optimal Latin hypercube design of experiments. International journal for numerical methods in engineering. 2010;82(2):135-56.

55. Giunta A, Wojtkiewicz S, Eldred M, editors. Overview of modern design of experiments methods for computational simulations. 41st Aerospace Sciences Meeting and Exhibit; 2003.

56. Park J, Lee KS, Kim MS, Jung D. Numerical analysis of a dual-fueled CI (compression ignition) engine using Latin hypercube sampling and multi-objective Pareto optimization. Energy. 2014;70:278-87.

57. Alsharif F, McNaughton Jr JL. Optimization Analysis of a V-Twin Motorcycle Engine Using WAVE Cycle Analysis and an iSight Optimization Framework. Ricardo software e-Brochure v3. 2005.

58. Tariq R, Sohani A, Xamán J, Sayyaadi H, Bassam A, Tzuc OM. Multi-objective optimization for the best possible thermal, electrical and overall energy performance of a novel perforated-type regenerative evaporative humidifier. Energy Conversion and Management. 2019;198:111802.

59. Sayyaadi H, Babaelahi M. Multi-objective optimization of a joule cycle for re-liquefaction of the Liquefied Natural Gas. Applied energy. 2011;88(9):3012-21.